Geophysical Research Letters

RESEARCH LETTER
10.1029/2019GL085455

Long-Term SST Variability on the Northwest Atlantic Continental Shelf and Slope

Zhuomin Chen[1,2], Young-Oh Kwon[1], Ke Chen[1], Paula Fratantoni[1,3], Glen Gawarkiewicz[1], and Terrence M. Joyce[1]

[1]Physical Oceanography Department, Woods Hole Oceanographic Institution, Woods Hole, MA, USA, [2]National Research Council Postdoctoral Associateship Program, Northeast Fisheries Science Center, Woods Hole, MA, USA, [3]NOAA NMFS, Northeast Fisheries Science Center, Woods Hole, MA

Key Points:
- Meridionally coherent surface warming is observed over the Northwest Atlantic continental shelf and slope
- The linear trends in SST exhibit distinct spatial maxima in the slope region off Georges Bank and Cape Hatteras
- Long-term variations in the meridional means of SST are highly correlated with basin-averaged values

Correspondence to:
Z. Chen,
zchen@whoi.edu

Citation:
Chen, Z., Kwon, Y.-O., Chen, K., Fratantoni, P., Gawarkiewicz, G., & Joyce, T. M. (2020). Long-term SST variability on the northwest Atlantic continental shelf and slope. *Geophysical Research Letters*, *47*, e2019GL085455. https://doi.org/10.1029/2019GL085455

Received 20 SEP 2019
Accepted 3 JAN 2020
Accepted article online 6 JAN 2020

Abstract The meridional coherence, connectivity, and regional inhomogeneity in long-term sea surface temperature (SST) variability over the Northwest Atlantic continental shelf and slope from 1982–2018 are investigated using observational data sets. A meridionally concurrent large SST warming trend is identified as the dominant signal over the length of the continental shelf and slope between Cape Hatteras in North Carolina and Cape Chidley, Newfoundland and Labrador, Canada. The linear trends are 0.37 ± 0.06 and 0.39 ± 0.06 °C/decade for the shelf and slope regions, respectively. These meridionally averaged SST time series over the shelf and slope are consistent with each other and across multiple longer observational data sets with records dating back to 1900. The coherence between the long-term meridionally averaged time series over the shelf and slope and basin-wide averaged SST in the North Atlantic implies approximately two thirds of the warming trend during 1982–2018 may be attributed to natural climate variability and the rest to externally forced change including anthropogenic warming.

Plain Language Summary This study investigates long-term changes in the sea surface temperature (SST) since 1982 over the Northwest Atlantic continental shelf and slope. In particular, we focus on the changes consistently found from Cape Hatteras, North Carolina, United States, to Cape Chidley, Newfoundland and Labrador, Canada. The SST warming rates concurrently found over this large latitudinal range are 0.37 ± 0.06 and 0.39 ± 0.06 °C/decade for the shelf and slope regions, respectively. Analysis indicates that approximately two thirds of the warming trend during 1982–2018 may be attributed to natural climate variability and the rest to externally forced change including anthropogenic warming. Our findings are further confirmed by comparing with multiple other observational data sets.

1. Introduction

The Northwest Atlantic (NWA) continental shelf and slope between Cape Hatteras and Labrador are dominated by equatorward flow, with relatively cold and fresh subpolar and Arctic-origin water (Labrador Shelf and Slope Currents) advected from the north (Fratantoni & Pickart, 2007; Loder et al., 1998). Further offshore in the open ocean, the Gulf Stream transports warm and salty water from the south, separating from the coast near Cape Hatteras and meandering northeastward. Warm-core rings form in the Slope Water region between the continental shelf and the Gulf Stream and propagate westward/southwestward before impinging on the shelf or reattaching to the Gulf Stream (e.g., Chen, He, et al., 2014; Joyce et al., 1984; Zhang & Gawarkiewicz, 2015). The NWA continental shelf and slope west of the tail of the Grand Banks are subject to influences from both the Labrador current and the Gulf Stream (e.g., Loder et al., 1998).

Sea surface temperature (SST) on the NWA continental shelf and slope exhibits significant variability on a broad range of time scales (Friedland & Hare, 2007; Richaud et al., 2016; Shearman & Lentz, 2010). In recent decades, accelerated warming trends on the NWA continental shelf have been detected in both surface and subsurface layers (Brickman et al., 2018; Forsyth et al., 2015; Pershing et al., 2015). There is evidence that this warming has had major impacts on marine ecosystems and fishery productivity, with commercial importance (Lucey & Nye, 2010; Mills et al., 2013; Mountain & Murawski, 1992; Nye et al., 2009; Pershing et al., 2015).

©2020. American Geophysical Union. All Rights Reserved.

Shearman and Lentz (2010) examined observations collected along the east coast of North America since the 1820s, concluding that long-term SST variations off the U.S. East Coast are dominated by along-shelf advection originating from Labrador rather than local air–sea heat exchange. On seasonal time scales, Richaud et al. (2016) reported that SST changes over the NWA continental shelf are mainly driven by surface heat flux and strongly correlated with latitude, based on in situ observations since the 1950s. Chen et al. (2015) used observational data and a high-resolution numerical model to show that an episode of extreme warming observed in 2012 was primarily driven by anomalous wintertime air–sea heat exchange. Further, a direct link was established between the behavior of the midlatitude jet stream and temperature anomalies over the northeast U.S. continental shelf (Chen, Gawarkiewicz, et al., 2014).

Most previous studies have examined long-term variability within smaller subregions, for example, the Gulf of Maine (GoM). However, given the interconnected nature of the system, we expect that improved understanding of the long-term variability can be gained from examining the region as a whole (Fratantoni & Pickart, 2007; Loder et al., 1998). Here, we investigate the long-term SST variability on the shelf and slope from the Labrador Shelf to Cape Hatteras, focusing on its coherence, connectivity, and regional differences.

2. Study Area, Data, and Methods

2.1. Study Area

This study examines SST on the NWA continental shelf and slope, between Cape Chidley, Newfoundland and Labrador, Canada, and Cape Hatteras, North Carolina (Figure 1). The shelf and slope regions are separated by the 200-m isobath. We further divide the region into smaller subregions, mostly based on physical environment and geography (Figure 1). The shelf region consists of 14 subregions, extending from the southern Mid-Atlantic Bight (MAB) to the Labrador Shelf. Among these, the first five shelf boxes nearly correspond to the Ecoregions of the Northeast U.S. shelf—the southern MAB, northern MAB, Georges Bank (GB), western GoM, and eastern GoM (Ecosystem Assessment Program, 2012). The Scotian Shelf (SS) is separated into two parts at 62°W: western SS (shelf box 06) and eastern SS (shelf box 07). The Gulf of St. Lawrence is separated into northern (shelf box 09) and southern (shelf box 08) regions along the Laurentian Channel. The remaining four shelf boxes along the Labrador Shelf north of the Newfoundland Shelf (NFL, box 10) are separated by the latitudes of 52°N, 54.67°N, and 57.83°N.

For the slope, we focus on the region between 35°N and 50°N, where slope processes have been shown to directly influence shelf temperatures on a variety of time scales (e.g., Chen, He, et al., 2014; Zhang & Gawarkiewicz, 2015; Gawarkiewicz et al., 2018). The slope region consists of eight subregions. The southern boundaries of slope boxes A through E are generally parallel to the main axis of the Gulf Stream, covering the slope sea between the continental shelf and the Gulf Stream. Results are not sensitive to slight northward or southward modification of the southern boundary. The southern boundaries of slope boxes F to H are aligned with the 4,000-m isobath. Slope boxes A to F are separated by longitudes ranging from 50°W to 70°W, with an interval of 5°. Slope boxes F to H are separated by latitudes of 43°N and 46°N.

2.2. SST Data Sets

We use a high-resolution satellite-derived data set—the ¼° National Oceanic and Atmospheric Administration Optimum Interpolation SST (NOAA OISST v2) data set (Reynolds et al., 2007)—to examine the temporal and spatial variability of SST across the shelf and slope regions in the NWA. SST is set to −1.8 °C where sea ice concentration is at least 90% (Reynolds et al., 2002). Results are not sensitive to masking in these ice-covered areas. The temporal range extends from 1982 to 2018, with monthly resolution. We used three other historical data sets for comparison, each having century-long temporal coverage dating back to at least 1900, though with coarser spatial resolutions. These include the Hadley Centre Sea Ice and SST (HadISST v1.1; Rayner et al., 2003), the Centennial *in situ* Observation-Based Estimates of SST (COBE SST; Ishii et al., 2005), and the NOAA Extended Reconstructed SST (NOAA ERSST v5; Huang et al., 2017). The HadISST and COBE SST have a 1° resolution, while the ERSST is on a 2° grid.

We also consider near-surface air temperature (usually at 2 m) records from coastal land-based stations (Figure 1) from the Global Historical Climatology Network-Monthly Database, version 4.0, archived at the National Centers for Environmental Information (https://www.ncdc.noaa.gov/; Menne et al., 2018). We only select stations located near the coast (within 100-km distance from the coast) between Cape Hatteras

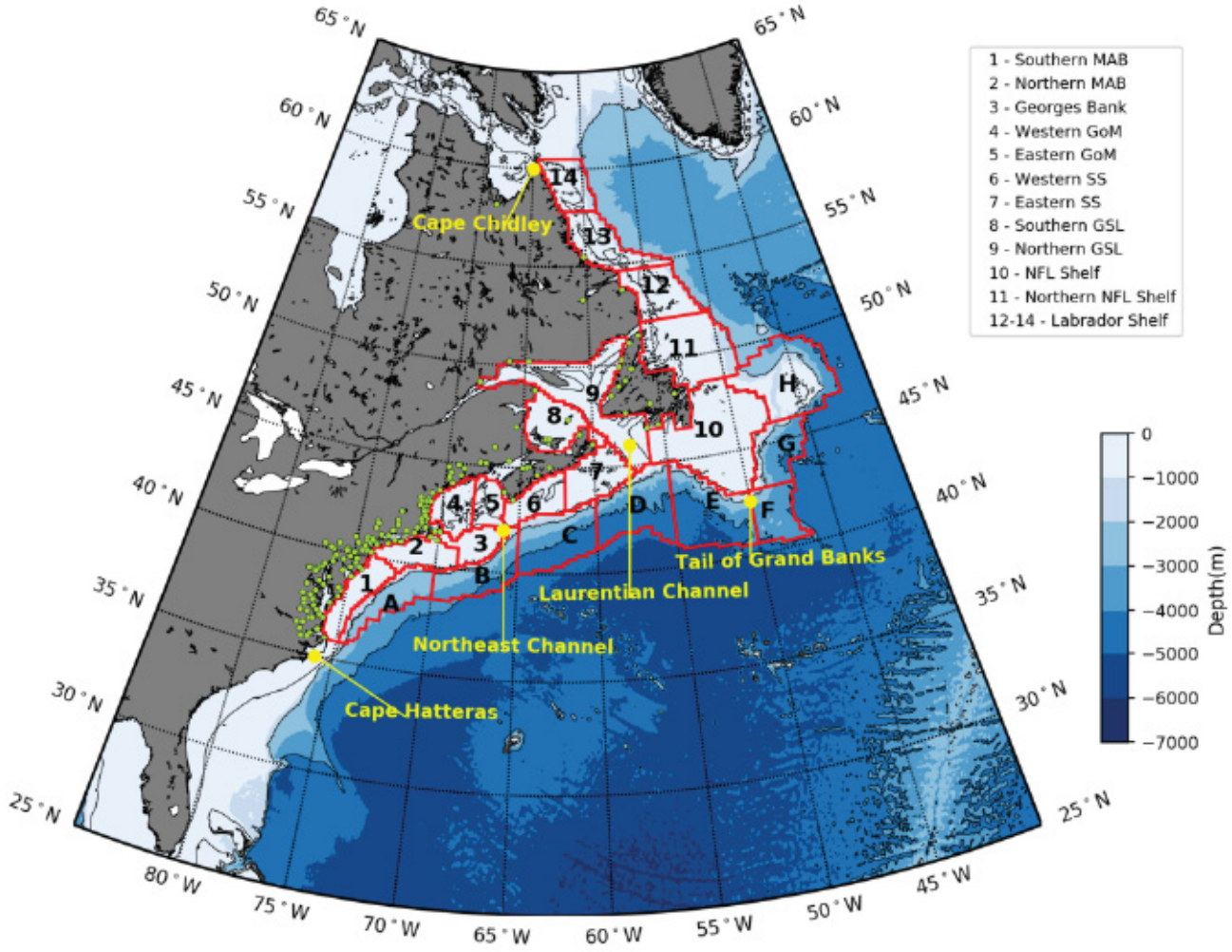

Figure 1. The Northwest Atlantic continental shelf and slope regions, bounded by the red lines. The shelf region consists of 14 shelf boxes (with numbers in black), which are named according to their geographic locations as illustrated in the legend (MAB, Mid-Atlantic Bight; GoM, Gulf of Maine; SS, Scotian Shelf; GSL, Gulf of St. Lawrence; and NFL, Newfoundland). The slope region consists of eight slope boxes (boxes A–H). The land-based stations measuring air temperature are marked as light green dots on the map. Major geographic locations are labeled. Three isobaths are plotted as thin black lines: 200 m, 2,000 m, and 4,000 m.

and the Labrador Shelf, with temporal coverage including 1982–2018 and measurement elevation less than 110 m. There are only four stations near the Labrador Shelf satisfying these conditions. To take into account the spatial inhomogeneity in air temperature observations, we have separated the observations into smaller regions, divided by 5° latitudinal increments. The average air temperature for each smaller region is calculated first, followed by an average calculated from the regional average air temperatures. The final meridional mean of the air temperature spans the same latitudinal range as the shelf and slope.

We calculated and plotted the Gulf Stream position using daily ¼° satellite-based gridded sea surface height for 1993–2018 from the Copernicus Marine Environment Monitoring Service (http://marine.copernicus.eu/). The average position of the Gulf Stream is identified at each longitude between 52° and 72°W, as the grid node where the standard deviation of sea level anomalies is maximized (Pérez-Hernández & Joyce, 2014). The average Gulf Stream path is nearly identical to the axis of maximum geostrophic velocity (not shown).

2.3. Methods

Monthly spatially averaged SST time series are calculated for each shelf and slope box, and a monthly mean climatology for the period 1982–2018 is subsequently removed to obtain SST anomaly (SSTA) time series within each box. Subsequently, yearly SSTA time series are calculated for each year. Similar methods were applied to obtain air temperature anomaly time series.

All the correlations are based on yearly time series. Statistical significance is calculated via a Student's t test considering the effective degree of freedom to account for autocorrelation (Bretherton et al., 1999). Linear regressions are used to calculate the linear trends, and the corresponding standard errors are calculated at the 5% level.

3. Results

3.1. Meridional Structure of Long-Term SST Variability

To investigate the meridional coherence and connectivity in the long-term SST variability over the NWA continental shelf and slope, the yearly SSTAs within each subregion are stacked in the meridional direction for the shelf and slope (Figures 2a and 2b). The most notable signal is relatively cool SSTA in the first half of the time series (before 1999) and relatively warm in the latter half (after 2005) for both the shelf and slope. These long-term warming signals are more or less meridionally coherent.

On top of the meridionally coherent warming trend, varying degrees of warming are observed among the shelf and slope subregions. The warming rates of each shelf and slope subregion are sensitive to the selection of the period. Generally, from 1982 to 2018, the northern regions of the shelf (shelf boxes 11–14) and slope (slope boxes F–H) exhibit relatively slow warming rates, especially slope box F, which has a slight cooling trend in recent decades. The fastest warming rates, based on the linear trends for each subregion, are observed in the SS and GoM and in slope boxes B–D. In addition, there are concurrent extreme signals in the meridional direction. Most notably, prominent warming is observed in 2012 across all latitudes, a signal attributed predominantly to anomalous wintertime air–sea heat flux (Chen, Gawarkiewicz, et al., 2014; Chen et al., 2015).

Figures 2a and 2b also hint at equatorward propagation of warm and cold anomalies, potentially due to along-shelf and slope advection. Cold anomalies in the northernmost shelf boxes in 1983–1984 propagate equatorward until 1987–1988, equivalent to a speed of 3–4 cm/s. This is consistent with the mean propagation speed (4 cm/s) estimated by the Marine Ecosystem Responses to Climate In the North Atlantic Working Group (2012) for the advection of salinity anomalies of the Arctic-originated waters along the continental shelf from the SS to the GoM/GB region. Similar results are found for the warm temperature anomalies in the shelf regions between 2010 and 2018. For some years, the southern and northern boxes have opposing thermal responses, for example, between slope boxes A–D and F–H from 2014 to 2018.

3.2. Meridionally Averaged Shelf and Slope SSTAs

Given the meridionally coherent temperature variability noted above, we calculated the SSTA for the entire shelf and the entire slope regions, generated the same way as was done for each single shelf/slope box (Figure 2c). The meridional mean shelf and slope SSTAs are highly coherent with each other throughout the record ($r = 0.85$ with trend; $r = 0.66$ after linearly detrended; both $p < 0.05$). Linear trends are 0.37 ± 0.06 °C/decade for the shelf region and 0.39 ± 0.06 °C/decade for the slope region. Removing the meridional mean from the SSTA time series within each individual subregion mostly eliminates the linear SSTA warming trends observed in the shelf and slope regions (not shown). In addition, the extreme warming in 2012 on both the shelf and slope disappears.

Assuming the coherent trends observed over the length of the study domain are driven primarily by the atmosphere, we compare meridional means for the shelf and slope with local near-surface air temperatures along the coast covering the same latitudinal range (Figure 1). The long-term trend in air temperature anomaly shows similar warming compared to the meridional mean shelf and slope SSTAs, although it is marginally smaller (0.39 ± 0.09 °C/decade; Figure 2d). The coastal air temperature anomaly is significantly correlated with the meridional mean of the shelf SSTA ($r = 0.81$; $p < 0.05$; detrended) but less correlated with the slope meridional mean SSTA ($r = 0.63$; $p < 0.05$; detrended). This suggests that the concurrent thermal signal over the shelf is more consistent with local atmospheric forcing than over the slope, although there are some exceptions. For example, warm atmospheric temperature anomalies during 1990, 1991, 1998, and 2010 did not coincide with warm SST anomalies, suggesting that ocean processes play an important role in cooling surface temperatures during these periods.

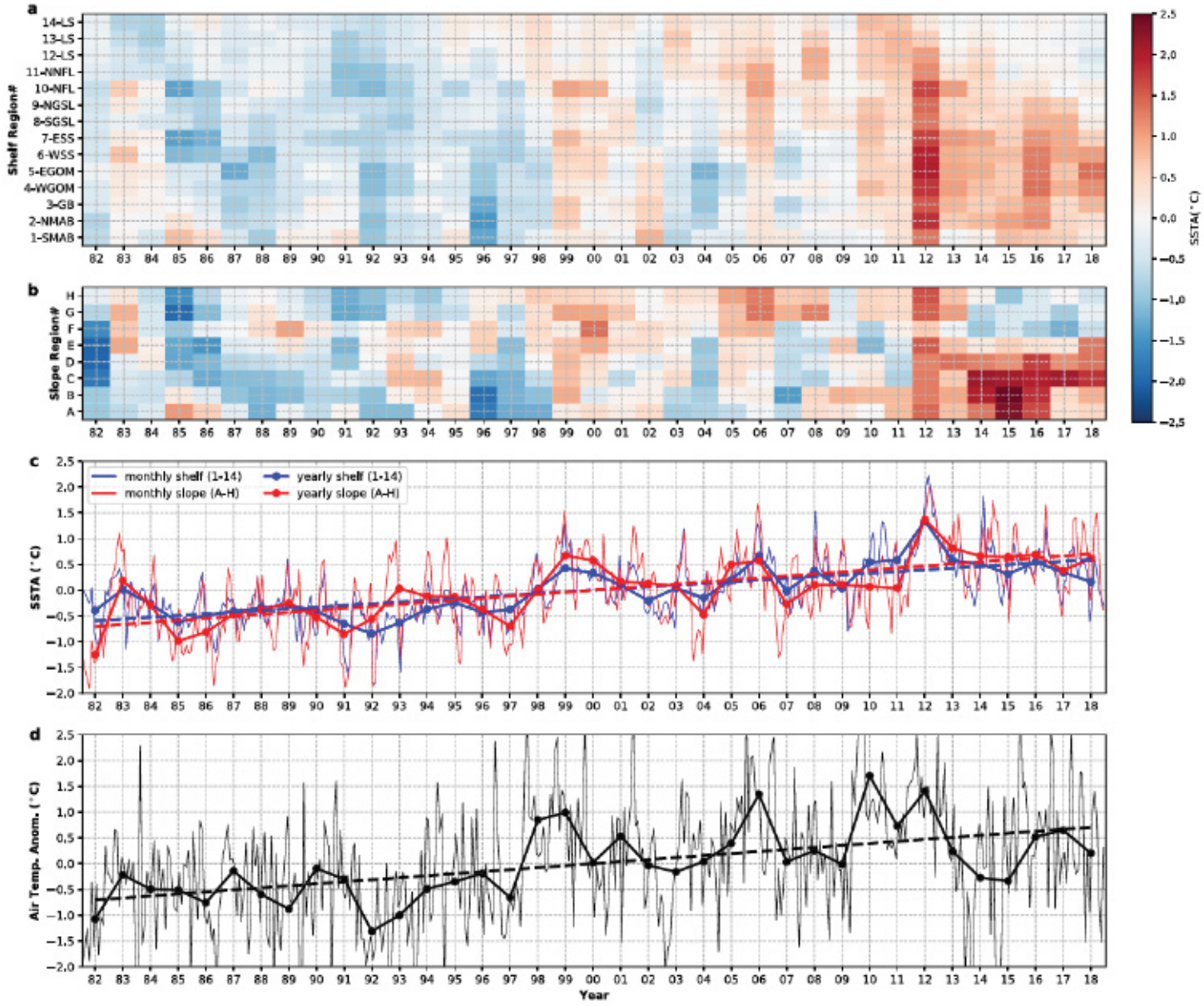

Figure 2. Time series of sea surface temperature anomalies (SSTA) and near-surface air temperature anomalies. (a) Hovmöller diagram of SSTA for the shelf boxes, with *x* axis representing year and *y* axis representing regional boxes in a latitudinally increasing order. (b) Same as (a) but for the slope boxes. (c) The meridional means for the shelf boxes 1–14 (blue) and slope boxes A–H (red), in monthly (thin solid lines) and yearly (thick solid lines) means. Linear trends are plotted as the thick dashed lines with corresponding colors. (d) The near-surface air temperature anomalies in monthly (thin solid black line) and yearly (thick solid black line) means based on air temperature observed near the coast over the land (cyan stars on Figure 1). The linear trend is plotted as the thick dashed black line.

3.3. Spatial Pattern of Linear Trends

On top of the meridionally coherent warming, there are considerable regional differences in the linear trends of SSTAs in the NWA (Figure 3). For example, the Labrador Shelf is warming slower (less than 0.25 °C/decade over shelf boxes 11–14) relative to the rest of the shelf, while the warming rate in the interior Labrador Sea is about 0.50 °C/decade, twice the warming trends on the Labrador Shelf.

Generally, the long-term linear trends on the shelf show less spatial variation than those over the slope where we observe distinct regions of warming and cooling (Figure 3). There are two prominent warming regions and one prominent cooling region within our study domain. One of the two warming regions is in slope boxes B to D, off the SS, GoM, and GB. The fastest surface warming measures roughly

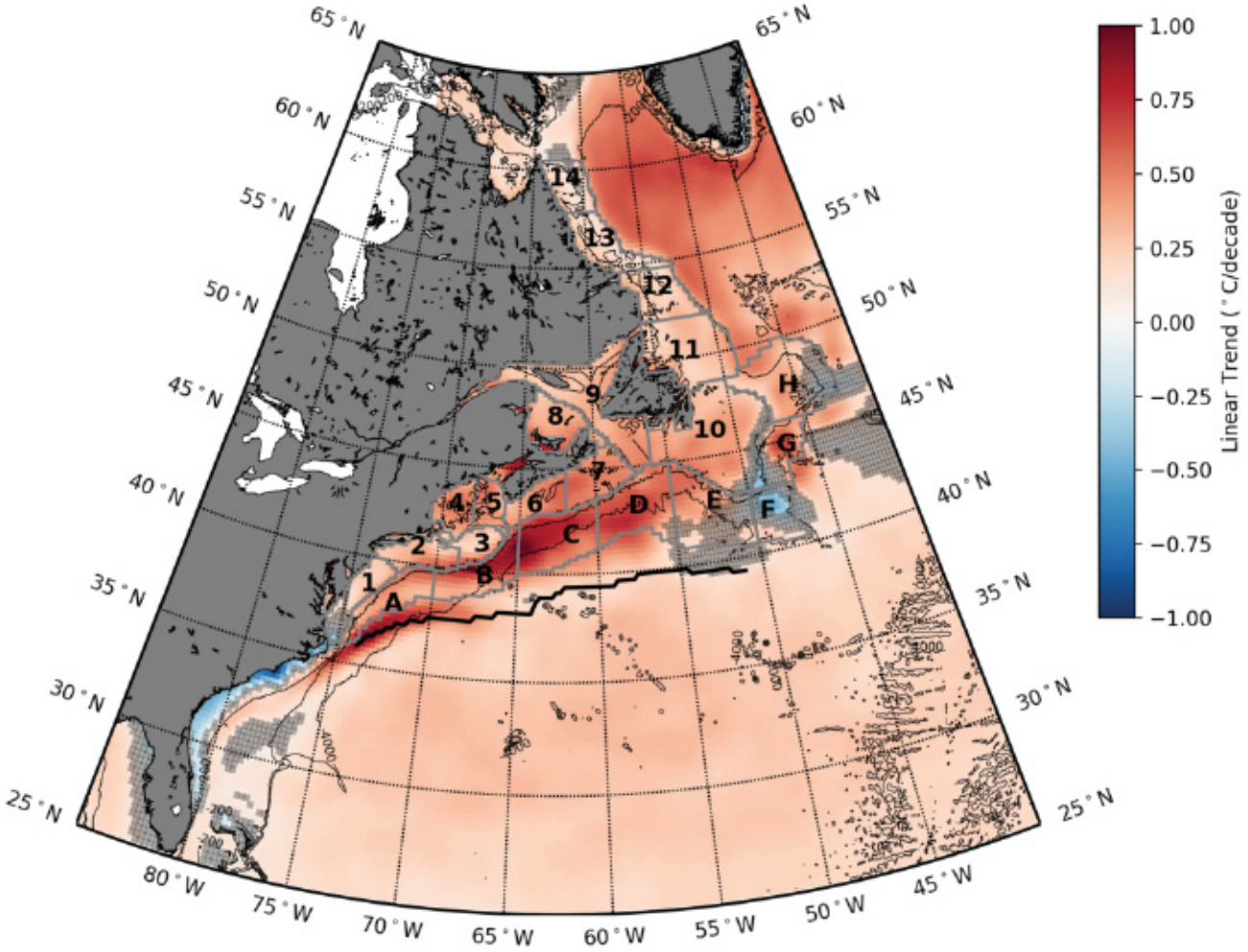

Figure 3. Spatial pattern of linear trends of sea surface temperature anomaly between 1982 and 2018 based on the National Oceanic and Atmospheric Administration Optimum Interpolation sea surface temperature. Insignificant values at 5% are masked in gray. The mean Gulf Stream path between 50° and 75°W is indicated by the black solid line. Three isobaths are plotted as thin black lines: 200 m, 2,000 m, and 4,000 m. The shelf and slope boxes are also indicated.

1.00 °C/decade over the slope between the 2,000- and 4,000-m isobaths off the Northeast Channel. Enhanced warming is also observed along the Gulf Stream mean path between 70° and 75°W, with a maximum value of 0.96 °C/decade. A region of enhanced cooling is observed over the slope near the tail of the Grand Banks between the 200- and 4,000-m isobaths, with the maximum cooling rate measuring 0.51 °C/decade. Another area of cooling is observed outside of our study region on the shelf in the South Atlantic Bight, where SST is cooling at a rate of about 1.01 °C/decade off Frying Pan Shoals.

4. Discussion

4.1. Meridionally averaged Long-Term SST Warming Trends

To assess the robustness of the long-term SST variability, we compared the results from the NOAA OISST with three other coarser resolution SST data sets. Despite different spatial resolutions, the meridional means of shelf and slope SSTAs in the three data sets show a similar behavior to those based on the NOAA OISST data set during the overlapping period (Figures 4a and 4b). The correlation coefficient between any pair among the four data sets is above 0.94 for the shelf and above 0.82 for the slope after linearly detrending the time series for 1982–2018.

Considering the longer period since the 1900s, the three additional data sets exhibit consistent long-term changes in the meridional means, especially for the continental shelf region. The correlation coefficients

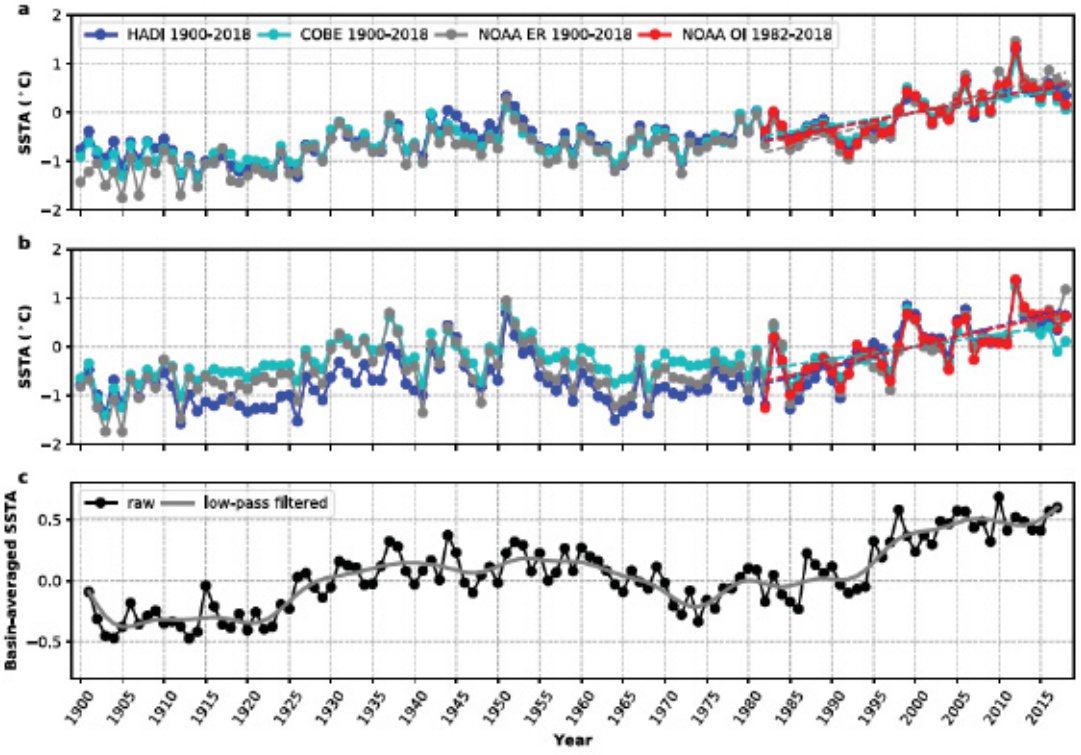

Figure 4. Comparison of meridional mean sea surface temperature (SST) anomalies time series for the overall shelf and slope regions, as well as the North Atlantic basin-averaged time series. (a) Comparison of meridional mean SST anomalies between four different observational data sets for the overall shelf region (shelf boxes 1–14): Hadley Centre Sea Ice and SST (HadISST; blue; 1900–2018), COBE SST (cyan; 1900–2018), National Oceanic and Atmospheric Administration Extended Reconstructed SST (NOAA ERSST; gray; 1900-2018), and NOAA Optimum Interpolation (OISST; red; 1982–2018); (b) Same as (a) but for the overall slope region (slope boxes A–H); (c) Basin-averaged annual sea surface temperature anomalies for the whole North Atlantic (0°–60°N and 0°–80°W) based on HadISST after masking out the sea-ice grid points, represented by the black solid line, and its 10-year low-pass filtered time series, represented by the thick solid gray line, between 1901 and 2017.

between any pair among the three data sets are always above 0.90 for 1900–2018. These longer records provide additional insight into the recent strong warming trend, observed since 1982. On multidecadal time scales, meridional means on the NWA continental shelf are cold before the 1930s, followed by a relatively warm period centered around the 1950s, consistent with lightship temperature records (Stearns, 1965). Another cold episode occurs between the 1960s and 1980s, followed by rapid warming in recent decades. This multidecadal variability is superimposed on an overall trend of warming. The linear trends for 1900–2018 in the meridional means of shelf SSTA are about 0.10 ± 0.01, 0.10 ± 0.01, and 0.14 ± 0.01 °C/decade for the three data sets, which are consistent with the previously reported long-term changes of SSTA in GoM (1.0 ± 0.3 °C/century) from 1820s to 2010 (Shearman & Lentz, 2010).

Over the continental slope, consistency among the three longer data sets decreases, mainly during the two cold episodes in the 1910s–1930s and 1960s–1980s. On average, the HadISST data set is about 0.62 °C and 0.53 °C colder than the COBE SST data set and 0.40 °C and 0.24 °C colder than the NOAA ERSST data set during these two periods, while the correlation coefficients between the HadISST and the other two are about 0.82 and 0.86 after detrending. The linear trends of three data sets in meridional means of SSTA over the slope are about 0.11 ± 0.01, 0.06 ± 0.01, and 0.09 ± 0.01 °C/decade, which also indicate the general increase of temperature since the 1900s. Similar to the 1982–2018 period, the meridional means on the shelf and slope are highly correlated in 1900–2018 ($r > 0.78$; $p < 0.05$; detrended).

The longer time series suggest that the strong warming trends on shelf and slope since 1982 are composed of at least two components, that is, the multidecadal variability and longer-term warming trend. The basin-wide averaged SSTA in the whole North Atlantic (0° to 60°N and 0° to 80°W) similarly exhibits two components (Figure 4c), which are interpreted by previous studies as the natural variability and externally forced warming trend, respectively (Frankignoul et al., 2017; Sutton et al., 2018; Trenberth & Shea, 2006;

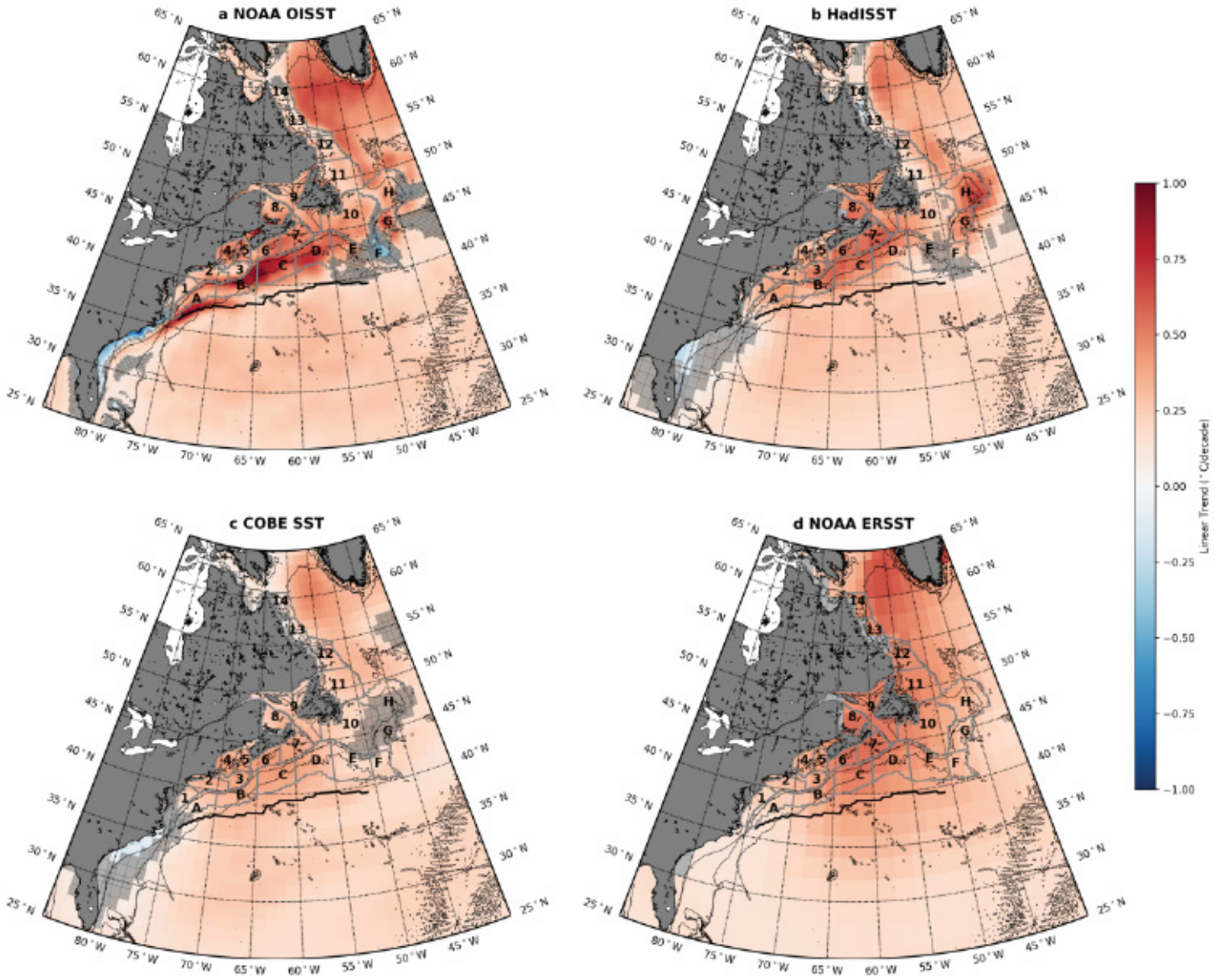

Figure 5. Comparison of spatial patterns in surface sea temperature (SST) linear trends (1982–2018) between four different data sets: (a) National Oceanic and Atmospheric Administration Optimum Interpolation SST (NOAA OISST), (b) Hadley Centre Sea Ice and SST (HadISST), (c) Centennial *in situ* Observation-Based Estimates of SST (COBE SST), and (d) NOAA Extended Reconstructed SST (ERSST). The Gulf Stream location, region boundaries, and numbers are the same as those in Figure 3. Insignificant values at 5% are masked in gray.

Ting et al., 2009). The multidecadal variability (emphasized with the 10-year low-pass filtered gray solid line in Figure 4c) is often called the Atlantic Multidecadal Variability or Atlantic Multidecadal Oscillation (Enfield et al., 2001; Kerr, 2000). A quadratic trend is fitted to the basin-wide time series for 1900–2018 as an approximate estimate for the externally forced signal (cf., Enfield & Cid-Serrano, 2010). This externally forced signal explains approximately one third of the linear trend in 1982–2018 of the basin-wide SSTA. We have also used a more sophisticated method to estimate the externally forced signal, which is an optimal perturbation filter based on linear inverse modeling (Frankignoul et al., 2017). The externally forced signal estimated from the second method also explains approximately one third of the linear trend in 1982–2018. The similarity between the basin-wide and shelf/slope SSTA time series ($r = 0.80$ for the shelf and $r = 0.77$ for the slope, both $p < 0.05$ including the long-term trends based on the HadISST; $r = 0.61$ after linearly detrending for both) suggests a similar decomposition for the shelf and slope SSTA.

Hence, approximately two thirds of the linear trend of SST anomalies in the shelf and slope region in 1982–2018 may be attributed to the natural multidecadal variability.

4.2. Ocean Processes Contributing to the Spatial Structure

Although the coherent simultaneous thermal signals (meridional means of SSTA) over the NWA continental shelf and slope suggest large-scale atmospheric forcing as the dominant driver, the spatial inhomogeneity in the linear trends of SSTA suggest that local ocean processes also play an important role. Based on the high-resolution NOAA OISST data set (1982-2018), the two regions with prominent warming trends observed over the slope are likely related to Gulf Stream variability. The Gulf Stream has been reported to have a slight northward shift during recent years (Joyce et al., 2019), which is correlated with changes in fish distribution over the shelf (Davis et al., 2017; Nye et al., 2009) and associated with warmer ocean temperature in the NWA Ocean (Frankignoul et al., 2001; Peña-Molino & Joyce, 2008; Zhang & Vallis, 2007). It is plausible that the enhanced warming trend concentrated along the Gulf Stream path is caused by a northward shift in the position of the Gulf Stream. On the other hand, the enhanced warming trends in the slope region off the SS, GoM, and GB may be related to an increase in the number of Gulf Stream warm-core rings in the region (Gangopadhyay et al., 2019) or the westward shift of the Gulf Stream destabilization point (Andres, 2016). The westward shift of the destabilization point increases the likelihood of Gulf Stream meanders and rings acting in the slope region. In these two regions, the correlation coefficients between the yearly SSTA and SSHA in 1993–2018 are 0.89 and 0.82 after linearly detrending, respectively, further suggesting the role of the Gulf Stream variability.

The localized cooling trends near the tail of Grand Banks may also be due to a slight offshore shift in the Gulf Stream path between 65°W and 50°W (Dong et al., 2019). This cooling pattern only exists in the high-resolution NOAA OISST data set, compared with the three coarser data sets (Figure 5). However, the enhanced warming pattern observed in the slope region is hinted at in the other data sets despite the overall weaker trends.

5. Conclusions

We investigated the coherence, connectivity, and regional differences in long-term SST variability from 1982–2018 over the NWA continental shelf and slope using several observational data sets. Given the large latitudinal extent of the study domain, extending from Labrador to Cape Hatteras, we divided the domain into subregions according to latitude and geography. Despite some spatial inhomogeneity in the long-term changes of SSTA, the leading signal is strong meridionally coherent long-term warming along the entire length of the shelf and slope. The linear trends in 1982–2018 are 0.37 ± 0.06 °C/decade for the shelf region and 0.39 ± 0.06 °C/decade for the slope region. These meridional means over the whole shelf and slope regions are consistent not only with each other but also with those computed using three coarser observational data sets extending back to the 1900s. We further compared these long-term SST changes with local near-surface air temperature anomalies over the land along the coast, which was highly correlated with the meridional mean of shelf SST. Since 1900, the long-term meridional means are highly coherent with the basin-averaged SST in the whole North Atlantic confounded by the multidecadal variability and overall longer-term warming trend. Finally, the similarity between the basin-wide average and the shelf/slope meridional mean trends implies approximately two-thirds of the linear warming trend in 1982–2018 may be attributed to natural climate variability and approximately one third to external forcing.

Acknowledgments
We are grateful to the Editor Dr. Kathleen Donohue and two anonymous reviewers. This work was supported by NOAA's Climate Program Office's Modeling, Analysis, Predictions, and Projections (MAPP) program (NA19OAR4320074). We acknowledge our participation in MAPP's Marine Prediction Task Force. The data of NOAA OISST used in this study are available at NOAA Earth System Research Laboratory (https://www.esrl.noaa.gov/psd/data/gridded/data.noaa.oisst.v2.highres.html). The HadISST data set is available at Met Office, Hadley Centre (https://www.metoffice.gov.uk/hadobs/hadisst/). The COBE SST and NOAA ERSST data sets are available at NOAA Earth System Research Laboratory's Physical Sciences Division (https://www.esrl.noaa.gov/psd/data/gridded/data.cobe.html; https://www.esrl.noaa.gov/psd/data/gridded/data.noaa.ersst.v5.html). The near-surface air temperature is available at Global Historical Climatology Network-Monthly Database (https://www.ncdc.noaa.gov/data-access/land-based-station-data/land-based-datasets/global-historical-climatology-network-monthly-version-4). The data of SSH are available at Copernicus Marine Environment Monitoring Service (http://marine.copernicus.eu/services-portfolio/access-to-products/?option=com_csw&view=details&product_id=SEALEVEL_GLO_PHY_L4_REP_OBSERVATIONS_008_047).

References

Andres, M. (2016). On the recent destabilization of the Gulf Stream path downstream of Cape Hatteras. *Geophysical Research Letters*, *43*, 9836–9842. https://doi.org/10.1002/2016GL069966

Bretherton, C. S., Widmann, M., Dymnikov, V. P., Wallace, J. M., & Bladé, I. (1999). The effective number of spatial degrees of freedom of a time-varying field. *Journal of Climate*, *12*(7), 1990–2009.

Brickman, D., Hebert, D., & Wang, Z. (2018). Mechanism for the recent ocean warming events on the Scotian Shelf of eastern Canada. *Continental Shelf Research*, *156*, 11–22.

Chen, K., Gawarkiewicz, G., Kwon, Y. O., & Zhang, W. G. (2015). The role of atmospheric forcing versus ocean advection during the extreme warming of the Northeast US continental shelf in 2012. *Journal of Geophysical Research: Oceans*, *120*, 4324–4339. https://doi.org/10.1002/2014JC010547

Chen, K., Gawarkiewicz, G. G., Lentz, S. J., & Bane, J. M. (2014). Diagnosing the warming of the Northeastern US Coastal Ocean in 2012: A linkage between the atmospheric jet stream variability and ocean response. *Journal of Geophysical Research: Oceans*, *119*, 218–227. https://doi.org/10.1002/2013JC009393

Chen, K., He, R., Powell, B. S., Gawarkiewicz, G. G., Moore, A. M., & Arango, H. G. (2014). Data assimilative modeling investigation of Gulf Stream warm core ring interaction with continental shelf and slope circulation. *Journal of Geophysical Research: Oceans, 119*, 5968–5991. https://doi.org/10.1002/2014JC009898

Davis, X. J., Joyce, T. M., & Kwon, Y. O. (2017). Prediction of silver hake distribution on the Northeast US shelf based on the Gulf Stream path index. *Continental Shelf Research, 138*, 51–64.

Dong, S., Baringer, M. O., & Goni, G. J. (2019). Slow down of the Gulf Stream during 1993-2016. *Scientific Reports, 9*(1), 6672. https://doi.org/10.1038/s41598-019-42820-8

Ecosystem Assessment Program. (2012). Ecosystem status report for the northeast shelf large marine ecosystem—2011. *US Dept. Commer, Northeast Fish Sci. Cent. Ref. Doc., 12*, 1-32.

Enfield, D. B., & Cid-Serrano, L. (2010). Secular and multidecadal warmings in the North Atlantic and their relationships with major hurricane activity. *International Journal of Climatology, 30*(2), 174–184.

Enfield, D. B., Mestas-Nuñez, A. M., & Trimble, P. J. (2001). The Atlantic multidecadal oscillation and its relation to rainfall and river flows in the continental US. *Geophysical Research Letters, 28*(10), 2077–2080.

Forsyth, J. S. T., Andres, M., & Gawarkiewicz, G. G. (2015). Recent accelerated warming of the continental shelf off New Jersey: Observations from the CMV Oleander expendable bathythermograph line. *Journal of Geophysical Research: Oceans, 120*, 2370–2384. https://doi.org/10.1002/2014JC010516

Frankignoul, C., de Coëtlogon, G., Joyce, T. M., & Dong, S. (2001). Gulf Stream variability and ocean–atmosphere interactions. *Journal of Physical Oceanography, 31*(12), 3516–3529.

Frankignoul, C., Gastineau, G., & Kwon, Y. O. (2017). Estimation of the SST response to anthropogenic and external forcing and its impact on the Atlantic multidecadal oscillation and the Pacific decadal oscillation. *Journal of Climate, 30*(24), 9871–9895.

Fratantoni, P. S., & Pickart, R. S. (2007). The western North Atlantic shelfbreak current system in summer. *Journal of Physical Oceanography, 37*(10), 2509–2533.

Friedland, K. D., & Hare, J. A. (2007). Long-term trends and regime shifts in sea surface temperature on the continental shelf of the northeast United States. *Continental Shelf Research, 27*(18), 2313–2328.

Gangopadhyay, A., Gawarkiewicz, G., Silva, E. N. S., Monim, M., & Clark, J. (2019). An observed regime shift in the formation of warm core rings from the Gulf Stream. *Scientific Reports, 9*(1), 1–9.

Gawarkiewicz, G., Todd, R. E., Zhang, W., Partida, J., Gangopadhyay, A., Monim, M. U. H., et al. (2018). The changing nature of shelf-break exchange revealed by the OOI Pioneer Array. *Oceanography, 31*(1), 60–70. https://doi.org/10.5670/oceanog.2018.110

Huang, B., Thorne, P. W., Banzon, V. F., Boyer, T., Chepurin, G., Lawrimore, J. H., et al. (2017). NOAA Extended Reconstructed Sea Surface Temperature (ERSST), Version 5. *NOAA National Centers for Environmental Information*.

Ishii, M., Shouji, A., Sugimoto, S., & Matsumoto, T. (2005). Objective analyses of sea-surface temperature and marine meteorological variables for the 20th century using ICOADS and the Kobe collection. *International Journal of Climatology, 25*(7), 865–879.

Joyce, T., Backus, R., Baker, K., Blackwelder, P., Brown, O., Cowles, T., et al. (1984). Rapid evolution of a Gulf Stream warm-core ring. *Nature, 308*(5962), 837–840. https://doi.org/10.1038/308837a0

Joyce, T. M., Kwon, Y. O., Seo, H., & Ummenhofer, C. C. (2019). Meridional Gulf Stream shifts can influence wintertime variability in the North Atlantic storm track and Greenland blocking. *Geophysical Research Letters, 46*, 1702–1708. https://doi.org/10.1029/2018GL081087

Kerr, R. A. (2000). A North Atlantic climate pacemaker for the centuries. *Science, 288*(5473), 1984–1985. https://doi.org/10.1126/science.288.5473.1984

Loder, J., Petrie, B., & Gawarkiewicz, G. (1998). The coastal ocean off northeastern North America: A large-scale view. *The Sea, 11*, 105–138.

Lucey, S. M., & Nye, J. A. (2010). Shifting species assemblages in the northeast US continental shelf large marine ecosystem. *Marine Ecology Progress Series, 415*, 23–33.

Menne, M. J., Williams, C. N., Gleason, B. E., Rennie, J. J., & Lawrimore, J. H. (2018). The Global Historical Climatology Network Monthly Temperature Dataset, Version 4. *Journal of Climate, 31*(24), 9835–9854.

MERCINA Working Group (2012). Recent Arctic climate change and its remote forcing of Northwest Atlantic shelf ecosystems. *Oceanography, 25*(3), 208–213. https://doi.org/10.5670/oceanog.2012.64

Mills, K. E., Pershing, A. J., Brown, C. J., Chen, Y., Chiang, F. S., Holland, D. S., et al. (2013). Fisheries management in a changing climate: Lessons from the 2012 ocean heat wave in the Northwest Atlantic. *Oceanography, 26*(2), 191–195.

Mountain, D. G., & Murawski, S. A. (1992). Variation in the distribution of fish stocks on the northeast continental shelf in relation to their environment, 1980–1989. In *ICES Mar. Sci. Symp* (Vol. 195, pp. 424-432).

Nye, J. A., Link, J. S., Hare, J. A., & Overholtz, W. J. (2009). Changing spatial distribution of fish stocks in relation to climate and population size on the Northeast United States continental shelf. *Marine Ecology Progress Series, 393*, 111–129.

Peña-Molino, B., & Joyce, T. M. (2008). Variability in the slope water and its relation to the Gulf Stream path. *Geophysical Research Letters, 35*, L03606. https://doi.org/10.1029/2007GL032183

Pérez-Hernández, M. D., & Joyce, T. M. (2014). Two modes of Gulf Stream variability revealed in the last two decades of satellite altimeter data. *Journal of Physical Oceanography, 44*(1), 149–163.

Pershing, A. J., Alexander, M. A., Hernandez, C. M., Kerr, L. A., Le Bris, A., Mills, K. E., et al. (2015). Slow adaptation in the face of rapid warming leads to collapse of the Gulf of Maine cod fishery. *Science, 350*(6262), 809–812. https://doi.org/10.1126/science.aac9819

Rayner, N. A. A., Parker, D. E., Horton, E. B., Folland, C. K., Alexander, L. V., Rowell, D. P., et al. (2003). Global analyses of sea surface temperature, sea ice, and night marine air temperature since the late nineteenth century. *Journal of Geophysical Research, 108*(D14), 4407. https://doi.org/10.1029/2002JD002670

Reynolds, R. W., Rayner, N. A., Smith, T. M., Stokes, D. C., & Wang, W. (2002). An improved in situ and satellite SST analysis for climate. *Journal of Climate, 15*(13), 1609–1625.

Reynolds, R. W., Smith, T. M., Liu, C., Chelton, D. B., Casey, K. S., & Schlax, M. G. (2007). Daily high-resolution-blended analyses for sea surface temperature. *Journal of Climate, 20*(22), 5473–5496.

Richaud, B., Kwon, Y. O., Joyce, T. M., Fratantoni, P. S., & Lentz, S. J. (2016). Surface and bottom temperature and salinity climatology along the continental shelf off the Canadian and US East Coasts. *Continental Shelf Research, 124*, 165–181.

Shearman, R. K., & Lentz, S. J. (2010). Long-term sea surface temperature variability along the US East Coast. *Journal of Physical Oceanography, 40*(5), 1004–1017.

Stearns, F. (1965). Sea-surface temperature anomaly study of records from Atlantic coast stations. *Journal of Geophysical Research, 70*(2), 283–296.

Sutton, R. T., McCarthy, G. D., Robson, J., Sinha, B., Archibald, A. T., & Gray, L. J. (2018). Atlantic multidecadal variability and the UK ACSIS Program. *Bulletin of the American Meteorological Society*, *99*(2), 415–425.

Ting, M., Kushnir, Y., Seager, R., & Li, C. (2009). Forced and internal twentieth-century SST trends in the North Atlantic. *Journal of Climate*, *22*(6), 1469–1481.

Trenberth, K. E., & Shea, D. J. (2006). Atlantic hurricanes and natural variability in 2005. *Geophysical Research Letters*, *33*, L12704. https://doi.org/10.1029/2006GL026894

Zhang, R., & Vallis, G. K. (2007). The role of bottom vortex stretching on the path of the North Atlantic western boundary current and on the northern recirculation gyre. *Journal of Physical Oceanography*, *37*(8), 2053–2080.

Zhang, W. G., & Gawarkiewicz, G. G. (2015). Dynamics of the direct intrusion of Gulf Stream ring water onto the Mid-Atlantic Bight shelf. *Geophysical Research Letters*, *42*, 7687–7695. https://doi.org/10.1002/2015GL065530